This article has been accepted for publication in a future issue of this journal, but has not been fully edited. Content may change prior to final publication. Citation information: DOI 10.1109/TPWRS.2021.3062203, IEEE Transactions on Power Systems

Scalable Security-Constrained Unit Commitment under Uncertainty via Cone Programming Relaxation

Edward Quarm Jnr. and Ramtin Madani

***Abstract*—This paper is concerned with the problem of Security-Constrained Unit Commitment (SCUC) which is a long-standing challenge in power system engineering faced by system operators and utility companies on a daily basis. We consider a detailed variant of this problem that suffers from complexities posed by the presence of binary variables, the uncertainty of renewable sources and security constraints. A convex relaxation is formulated which is capable of finding feasible solutions within a provable distance from global optimality. We demonstrate the performance of this approach on detailed and challenging instances of SCUC with IEEE and PEGASE benchmark cases from MATPOWER [1]. The proposed approach is able to handle over 12,000 binary variables and 2 million continuous variables with significant improvement in solution quality over commonly-used off-the-shelf solvers and other methods of convex relaxation.**

***Index Terms*—Power generation scheduling, Power system security, Optimization methods**

I. Introduction

Unit commitment (UC) is the problem of determining the schedule and level of contributions by generators in a power grid to meet forecasted demand for electricity as economically as possible. The efficiency of wholesale power markets is highly dependent on solution methods for UC. Efficient algorithms based on high-fidelity power grid models can alleviate a variety of problems such as uplift payments, underfunded transmission rights and occasional disputes between market participants [2], [3]. Several variants of UC have been studied in the literature to address considerations such as contingency constraints and to mitigate the uncertainty of demand and renewable sources. Network components are prone to various sources of failure. Hence, contingency planning is central to reliable functioning of power grids. To ensure immunity to the outage of individual grid components, it is common-practice to impose a comprehensive list of constraints, accounting for pre-determined contingencies. This problem is regarded as Security-Constrained Unit Commitment (SCUC). Due to the ever increasing integration of renewable energy sources, several papers have considered stochastic formulations of SCUC to mitigate the risks associated with grid uncertainty. In this paper, we propose a computational method for SCUC under the uncertainty of renewable sources.

The presence of binary variables pose a major challenge in solving large-scale unit commitment problems. Therefore, a variety of methods have been developed for UC since the late 1960s. Among early attempts were rudimentary methods such as exhaustive enumeration and priority list [4]–[8] that are only applicable to small instances of UC. In the 1960s and 70s a number of Dynamic Programming (DP) methods were proposed for UC in [9]–[11], without success on large-scale problems due to curse of dimensionality. To this date, Lagrangian Relaxation (LR) has remained one of the successful methods to approach UC [12]–[14]. LR works by decomposing UC problems into a master problem and subproblems that are solved iteratively until an optimal solution is found. The success of LR is due to its reliance on a lower complexity dual formulation as opposed to the high dimensional primal UC problem which is tackled by other methods. Recent papers employ benders decomposition for separating the UC into master and subproblems to be solved using augmented LR or combined with DP and Genetic Algorithm (GA) [15]–[17] to achieve reasonable computational speed, though not fast enough for practical applications.

With the increase in computer memory and processing power Mixed-Integer Programming (MIP) methods such as Branch and Bound (B&B) have gained popularity as solution approaches to UC [18], [19]. Recently, MIP solvers such as CPLEX and GUROBI have become very popular and widely used to solve UC problems for commercial applications [2]. However, a main disadvantage of B&B is the rapid growth of search trees with the number of binary variables [20]. The success of MIP solvers in tackling stochastic SCUC problems depends on the tightness and compactness of formulation, number of binary variables, number of wind scenarios, number of contingencies and binding transmission line constraints [21]–[23]. In order to improve the efficiency and solution quality of B&B searches, the creators of CPLEX; IBM have offered improvements such as heuristics, node presolve and cutting planes [24]. Despite these improvements, a number of papers have reported that the computational burden on off-the-shelf MIP solvers increases when applied to large-scale SCUC problems as solvers either exceed the time-limit or CPU memory limit [21]–[23]. Many papers have also offered partial convex hull characterizations of UC feasible sets [25]–[28] to improve efficiency of B&B. The paper [29] offers a critical review of the common-practice of implementing linear programming (LP) relaxation as a reliable approach to UC.

Recently, more sophisticated convex relaxations such as Semidefinite Programming (SDP) and Second-Order Cone Programming (SOCP) have been used for solving different variants of UC [30], [31]. In [30], it is shown that perspective relaxation can significantly improve the performance of MIP search for UC. The paper [31] applies SDP relaxation to SCUC with AC network constraints. In [32] a strengthened SDP relaxation is proposed, which offers improved performance using the Reformulation Linearization Technique (RLT). The paper [33] employs SOCP to find globally optimal solutions

The authors are with the Department of Electrical Engineering, University of Texas at Arlington (email: edwardarthur.quarmjnr@uta.edu, ramtin.madani@uta.edu). This work is funded, in part, by the the National Science Foundation under award ECCS-1809454.

0885-8950 (c) 2021 IEEE. Personal use is permitted, but republication/redistribution requires IEEE permission. See http://www.ieee.org/publications_standards/publications/rights/index.html for more information.
Authorized licensed use limited to: University of Texas at Arlington. Downloaded on April 01,2021 at 15:39:46 UTC from IEEE Xplore. Restrictions apply.

This article has been accepted for publication in a future issue of this journal, but has not been fully edited. Content may change prior to final publication. Citation information: DOI 10.1109/TPWRS.2021.3062203, IEEE Transactions on Power Systems

to UC with AC network constraints. Due to the computational complexity of UC, solutions obtained from any polynomial-solvable relaxation may not be feasible for the original non-convex UC problem. To address this issue, the paper [34] proposes a sequential penalization method for UC to obtain near-globally optimal solutions.

This paper examines the complexity of tackling challenging day-ahead scheduling problems in cases where large-scale UC is combined with security constraints, contingency events and uncertain wind scenarios. We adopted a stochastic approach proposed in [35]. The base case and contingency states are tied together by generator ramp limits. In addition, generator re-dispatches are treated as recourse actions to contingencies. This stochastic approach to modeling system security is preferred to other modeling approaches because it allows for cost of each state to be weighted by its probability of occurrence.

In this paper, we leverage the power of SDP relaxation to alleviate the burden of branch-and-bound search for detailed and large-scale SCUC problems. While off-the-shelf SDP relaxation produces a lower bound on the optimal objective, it is computationally prohibitive thus not scalable [36], [37]. Hence, in this work, we are forging a low-complexity conic relaxation that is capable of solving large-scale SCUC. This effort is aligned with the recent body of research devoted to scalable variants of semidefinite programming [38]. In lieu of computationally demanding constraints, we employ low-order SDP constraints to determine binary variables. So as to strengthen the relaxation, valid inequalities are introduced from the multiplication of constraints through the Reformulation-Linearization Technique (RLT). To address cases for which the proposed relaxation is not exact, we propose a heuristic approach to infer near-globally optimal points from the outcome of convex relaxation. The proposed approach is tested on modified IEEE and PEGASE benchmark systems with realizations of uncertain wind scenarios and N-1 contingencies. The largest benchmark system considered includes 12,240 binary decision variables and 1,830,560 continuous variables. The performance of the proposed convex relaxation is compared with off-the-shelf solvers such as CPLEX and GUROBI and other methods of relaxation like perspective and LP relaxations.

The remainder of this paper is organized as follows. In Section II-A, we formulate the SCUC problem under uncertainty. This non-convex problem is convexified by means of convex surrogates in Section III. Next, a scalable convex relaxation is proposed in Section III to tackle SCUC in polynomial time. Section IV proposes a heuristic approach to infer near-globally optimal points from the outcome of convex relaxation. Extensive experiments are conducted in Section V on IEEE and PEGASE benchmark systems. Section VI concludes the paper.

A. Notations

Throughout this paper, matrices, vectors and scalars are represented by boldface uppercase, boldface lowercase and italic lowercase letters, respectively. $|\cdot|$ represents the absolute value of a scalar or the cardinality of a set. The symbol $(\cdot)^\top$ represents the transpose operator. The notation real$\{\cdot\}$ represents the real part of a scalar or a matrix. Given a matrix $\boldsymbol{A}$, the notation $\boldsymbol{A}_{jk}$ refers to its $(j,k)^{th}$ element. $\boldsymbol{A} \succeq 0$ means that $\boldsymbol{A}$ is symmetric and positive semidefinite.

II. Unit Commitment Problem

This work considers a secure unit commitment problem under wind generation uncertainty. As mentioned in the introduction, security constraints are modeled using a stochastic approach proposed in [35]. Contingencies in the network are modeled by specifying outages to units or lines. Locational reserve requirements are endogenously determined as a function of the set of included credible contingencies, which is in stark contrast to deterministic approach where zonal reserve requirements are predefined by system operators and employed in various UC studies [15]. Pre-defined or fixed reserve requirements are not used in this study, conversely we make use of generator ramp rate modeled after [39]. Also, we define a power contract variable which represents reference dispatch value from which dispatch deviations are defined.

Uncertainty in wind generation is modeled as scenarios with continuous probability distributions, such that each scenario represents a different forecast of wind. Furthermore, a transition probability matrix is used to describe the transitions from a limited set of base scenarios in one period to a limited set of base scenarios in the next period. Experimental data on generator and wind parameters including ramp rate for IEEE and PEGASE benchmark systems are specified in Section V.

A. Problem Formulation

The goal of unit commitment is to schedule the generation of electricity within a time horizon $\mathcal{T} = \{1, 2, \ldots, |\mathcal{T}|\}$. For every $t \in \mathcal{T}$, let $\mathcal{S}_t$ represent the set of all possible uncertainty scenarios for renewable sources at time t. Additionally, let $\mathcal{G}_t$ represent the set of all generating units that are available at time $t \in \mathcal{T}$. For every, $t \in \mathcal{T}$ and $s \in \mathcal{S}_t$, define $\mathcal{C}_{ts}$ as the set of all contingency cases with $0 \in \mathcal{C}_{ts}$ representing the base case (normal operation). Lastly, $\mathcal{G}_{tsc} \subseteq \mathcal{G}_t$ is defined as the set of all generating units that are available at time $t \in \mathcal{T}$, scenario $s \in \mathcal{S}_t$ and contingency $c \in \mathcal{C}_{ts}$, such that

$$\mathcal{G}_t = \cup_{s\in\mathcal{S}_t} \cup_{c\in\mathcal{C}_{ts}} \mathcal{G}_{tsc}.$$

Consider a power system with $\mathcal{V}$ as the set of buses, and $\mathcal{E}_{tc} \subseteq \mathcal{V} \times \mathcal{V}$ as the set of branches at time $t \in \mathcal{T}$ and contingency $c \in \cup_{s\in\mathcal{S}_t}\mathcal{C}_{ts}$.

Motivated by [35], we formulate SCUC using the following list of decision variables:

$$\{x_{tg} \in \{0,1\}\}_{t\in\mathcal{T},\, g\in\mathcal{G}_t},$$
$$\{p_{tg}^{\text{contract}},\ r_{tg}^{+},\ r_{tg}^{-},\ w_{tg}^{+},\ w_{tg}^{-} \in \mathbb{R}\}_{t\in\mathcal{T},\, g\in\mathcal{G}_t}$$
$$\{p_{tgsc}\}_{t\in\mathcal{T},\, g\in\mathcal{G}_t,\, s\in\mathcal{S}_t,\, c\in\mathcal{C}_{ts}}, \quad \{\boldsymbol{\theta}_{tsc} \in \mathbb{R}^{|\mathcal{V}|}\}_{t\in\mathcal{T},\, s\in\mathcal{S}_t,\, c\in\mathcal{C}_{ts}}.$$

Each x_{tg} is a binary variable indicating the on/off status of unit $g \in \mathcal{G}_t$ at time $t \in \mathcal{T}$ and p_{tg}^{contract} is its contract active power quantity. Variables (r_{tg}^{+}, r_{tg}^{-}) are upward and

0885-8950 (c) 2021 IEEE. Personal use is permitted, but republication/redistribution requires IEEE permission. See http://www.ieee.org/publications_standards/publications/rights/index.html for more information.
Authorized licensed use limited to: University of Texas at Arlington. Downloaded on April 01,2021 at 15:39:46 UTC from IEEE Xplore. Restrictions apply.

This article has been accepted for publication in a future issue of this journal, but has not been fully edited. Content may change prior to final publication. Citation information: DOI 10.1109/TPWRS.2021.3062203, IEEE Transactions on Power Systems

downward contingency reserve quantities, and (w^+_{tg}, w^-_{tg}) represent upward and downward load-following ramping reserve quantities, respectively. If $g \notin \mathcal{G}_t$, then

$$x_{tg} = p^{\text{contract}}_{tg} = r^+_{tg} = r^-_{tg} = w^+_{tg} = w^-_{tg} = 0.$$

Each variable p_{tgsc} denotes the active power injection at time $t \in \mathcal{T}$ by generator $g \in \mathcal{G}_t$, in scenario $s \in \mathcal{S}_t$ and contingency $c \in \mathcal{C}_{ts}$. Lastly, $\boldsymbol{\theta}_{tsc} \in \mathbb{R}^{|\mathcal{V}|}$ represents the vector of nodal phase angles at time $t \in \mathcal{T}$, scenario $s \in \mathcal{S}_t$ and contingency $c \in \mathcal{C}_{ts}$.

B. Objective function

We consider a holistic objective accounting for the expected value of the total cost throughout the time horizon $\mathcal{T}$, and across the set of all scenarios and contingencies. This objective is made up of the expected base case and post-contingency generation costs, ramping "wear and tear" costs, load-following ramp reserve and contingency reserve costs, as well as the generator start-up, shutdown and fixed costs. This objective function can be cast with respect to the following three expressions:

$$\sum_{t\in\mathcal{T}} \gamma_t \sum_{g\in\mathcal{G}_t} \sigma^{(1)}_{tg}(x_{tg}, r^+_{tg}, r^-_{tg}, w^+_{tg}, w^-_{tg}) \tag{1a}$$

$$\sum_{t\in\mathcal{T}} \sum_{s\in\mathcal{S}_t} \sum_{c\in\mathcal{C}_{ts}} \psi_{tsc} \sum_{g\in\mathcal{G}_{tsc}} \sigma^{(2)}_{tg}(p_{tgsc}, p^{\text{contract}}_{tg}) \tag{1b}$$

$$\sum_{t\in\mathcal{T}} \gamma_t \sum_{s_1\in\mathcal{S}_{t-1}} \sum_{s_2\in\mathcal{S}_t} \phi_{ts_1s_2} \sum_{g\in\mathcal{G}_{ts_20}} \sigma^{(3)}_{g}(p_{tgs_20}, p_{(t-1)gs_10}) \tag{1c}$$

In the first line of the objective (1a), the cost function $\sigma^{(1)}_{tg}$is defined as

$$\begin{aligned}
\sigma^{(1)}_{tg}(x_{tg}, r^+_{tg}, r^-_{tg}, w^+_{tg}, w^-_{tg}) \triangleq\ & \zeta_{tg}\ x_{tg} && \text{(2a)}\\
& + \zeta^{\uparrow}_{tg}\ (1 - x_{(t-1)g}) x_{tg} && \text{(2b)}\\
& + \zeta^{\downarrow}_{tg}\ x_{(t-1)g}(1 - x_{tg}) && \text{(2c)}\\
& + (\eta^+_{tg}\ r^+_{tg} + \eta^-_{tg}\ r^-_{tg}) && \text{(2d)}\\
& + (\mu^+_{tg}\ w^+_{tg} + \mu^-_{tg}\ w^-_{tg}) && \text{(2e)}
\end{aligned}$$

with the expressions (2a), (2b) and (2c) corresponding to generator fixed, startup and shutdown costs, respectively; while (2d) and (2e) account for the cost of contingency and load-following ramping reserves, respectively. The start-up and shutdown costs $\zeta^{\uparrow}_{tg}$ and $\zeta^{\downarrow}_{tg}$ incur with every time slot at which the unit changes status. The fixed production cost ζ_{tg} is enforced if the unit is active. The coefficients η^+_{tg} and η^-_{tg} are the costs incurred when reserves are purchased from a generating unit in the event of a contingency. The coefficients μ^+_{tg} and μ^-_{tg} are the costs incurred due to variations of active power between two consecutive time slots in which the unit g is committed. These costs are weighted by γ_t, which is the probability of transitioning to period t without branching off from the central base case path to a contingency.

In the second line (1b), the function $\sigma^{(2)}_{tg}(\cdot,\cdot)$ is defined as

$$\sigma^{(2)}_{tg}(p_{tgsc}, p^{\text{contract}}_{tg}) \triangleq \alpha^{\text{sqr}}_{tg}\ p^2_{tgsc} + \alpha^{\text{lin}}_{tg}\ p_{tgsc} + \tag{3a}$$

$$\frac{\beta^+_{tg}+\beta^-_{tg}}{2}\,|p_{tgsc} - p^{\text{contract}}_{tg}| + \frac{\beta^+_{tg}-\beta^-_{tg}}{2}(p_{tgsc} - p^{\text{contract}}_{tg}) \tag{3b}$$

including the quadratic expression (3a) with nonnegative quadratic and linear coefficients α^{sqr}_{tg} and α^{lin}_{tg}, and the term (3b) for assigning costs to deviations from contract values with nonnegative coefficients β^+_{tg} and β^-_{tg}. These costs are weighted by the probability of contingency ψ_{tsc}.

Finally, we have the third term (1c) representing a quadratic load-following ramp "wear and tear" cost

$$\sigma^{(3)}_{g}(p_{tgs_20}, p_{(t-1)gs_10}) \triangleq \kappa_g \times (p_{tgs_20} - p_{(t-1)gs_10})^2 \tag{4}$$

weighted by γ_t, the nonnegative coefficients κ_g, and $\phi_{ts_1s_2}$ which is the probability of transitioning to scenario s_2 in period t provided that scenario s_1 was realized in period $t-1$.

C. Constraints

We apply the following constraints which can be separated into five main categories:

1) Integrality constraints: For every $t \in \mathcal{T}$ and $g \in \mathcal{G}_t$, the binary requirements are:

$$x_{tg} \in \{0, 1\} \tag{5}$$

These constraints are the main sources of complexity in SCUC. We will relax the integrality constraints (5) and implicitly impose them via proxy conic and linear inequalities.

2) Unit capacity constraints: For every $t \in \mathcal{T}$ and $g \in \mathcal{G}_t$, the unit capacity constraints consist of:

$$\underline{p}_g\ x_{tg} \le p_{tgsc} \le \bar{p}_g\ x_{tg} \qquad \forall s \in \mathcal{S}_t,\ \forall c \in \mathcal{C}_{ts} \tag{6}$$

Constraint (6) ensures that when unit $g \in \mathcal{G}_t$ is committed during the interval t, then its active power injections lies within the pre-specified limits $\underline{p}_{tgsc}$ and $\bar{p}_{tgsc}$.

3) Minimum up/down time constraints: For every $t \in \mathcal{T}$ and $g \in \mathcal{G}_t$, the Minimum up/down time constraints are:

$$x_{tg} \ge x_{\tau g} - x_{(\tau-1)g} \quad \forall \tau \in \{t - m^{\uparrow}_g + 1, \ldots, t\} \tag{7a}$$

$$1 - x_{tg} \ge x_{(\tau-1)g} - x_{\tau g} \quad \forall \tau \in \{t - m^{\downarrow}_g + 1, \ldots, t\} \tag{7b}$$

where $m^{\uparrow}_g$ and $m^{\downarrow}_g$ denote the minimum up and down time limits of generator t, respectively.

4) Ramp constraints: For every $t \in \mathcal{T}$ and $g \in \mathcal{G}_t$, the generator ramp constraints consist of:

$$0 \le w^+_{tg} \le \bar{w}_{tg}, \tag{8a}$$

$$0 \le w^-_{tg} \le \underline{w}_{tg}, \tag{8b}$$

$$p_{tgs_20} - p_{(t-1)gs_10} \le w^+_{(t-1)g}, \quad \forall s_1 \in \mathcal{S}_{t-1},\ \forall s_2 \in \mathcal{S}_t \tag{8c}$$

$$p_{(t-1)gs_10} - p_{tgs_20} \le w^-_{(t-1)g}, \quad \forall s_1 \in \mathcal{S}_{t-1},\ \forall s_2 \in \mathcal{S}_t \tag{8d}$$

Constraints (8a)–(8b) impose the limits $\bar{w}_{tg}$ and $\underline{w}_{tg}$ on the upward and downward load-following reserve quantities of generator t, respectively. Constraints (8c)–(8d) limit changes in active power injection between two consecutive time slots during which the unit t is committed.

0885-8950 (c) 2021 IEEE. Personal use is permitted, but republication/redistribution requires IEEE permission. See http://www.ieee.org/publications_standards/publications/rights/index.html for more information.
Authorized licensed use limited to: University of Texas at Arlington. Downloaded on April 01,2021 at 15:39:46 UTC from IEEE Xplore. Restrictions apply.

This article has been accepted for publication in a future issue of this journal, but has not been fully edited. Content may change prior to final publication. Citation information: DOI 10.1109/TPWRS.2021.3062203, IEEE Transactions on Power Systems

5) Post-contingency reserve constraints: For every $t \in \mathcal{T}$ and $g \in \mathcal{G}_t$, the post-contingency reserve constraints are:

$$0 \le r^+_{tg} \le \bar{r}_{tg}, \tag{9a}$$
$$0 \le r^-_{tg} \le \underline{r}_{tg}, \tag{9b}$$
$$p_{tgsc} - p^{\text{contract}}_{tg} \le r^+_{tg}, \qquad \forall s \in \mathcal{S}_t,\ \forall c \in \mathcal{C}_{ts} \tag{9c}$$
$$p^{\text{contract}}_{tg} - p_{tgsc} \le r^-_{tg}, \qquad \forall s \in \mathcal{S}_t,\ \forall c \in \mathcal{C}_{ts} \tag{9d}$$
$$-\underline{\Delta}_g \le p_{tgsc} - p_{tgs0} \le \bar{\Delta}_g, \qquad \forall s \in \mathcal{S}_t,\ \forall c \in \mathcal{C}_{ts} \tag{9e}$$

Constraints (9a)–(9b) impose the upward/downward reserve capacity limits $\bar{r}_{tg}$ and $\underline{r}_{tg}$ on post-contingency dispatch quantities, respectively. Deviations from active power contract quantities are limited by constraints (9c)–(9d). Additionally, the constraint (9e) enforces the physical ramp limits $\underline{\Delta}_g$ and $\bar{\Delta}_g$ on downward and upward transitions from base to post-contigency cases.

6) DC network constraints: The DC modeling is employed to describe the flow of power throughout the network. To this end, let $\boldsymbol{B}$ denote the the imaginary part of the network bus admittance matrix and for each $t \in \mathcal{T}$ and $c \in \cup_{s\in\mathcal{S}_t}\mathcal{C}_{ts}$, let $\vec{\boldsymbol{B}}_{tc} \in \mathbb{R}^{|\mathcal{E}_{tc}|\times|\mathcal{V}|}$ and $\boldsymbol{B}_{tc} \in \mathbb{R}^{|\mathcal{V}|\times|\mathcal{V}|}$ represent the corresponding susceptance matrices. Additionally, define $\boldsymbol{C}_{tsc} \in \{0,1\}^{|\mathcal{G}_{tsc}|\times|\mathcal{V}|}$ as the incidence matrix whose (j,k) element is equal to 1, if and only if the unit g belongs to the bus k. For every $t \in \mathcal{T}$, the DC network constraints can be cast as

$$\boldsymbol{d}_{tc} + \boldsymbol{B}_{tc}\,\boldsymbol{\theta}_{tsc} = \boldsymbol{C}^\top_{tsc}\,\boldsymbol{p}_{tsc}, \quad \forall s \in \mathcal{S}_t,\ \forall c \in \mathcal{C}_{ts} \tag{10a}$$
$$|\vec{\boldsymbol{B}}_{tc}\,\boldsymbol{\theta}_{tsc} + \boldsymbol{f}^{\text{shift}}_{tc}| \le \boldsymbol{f}^{\max}_{tc} \quad \forall s \in \mathcal{S}_t,\ \forall c \in \mathcal{C}_{ts} \tag{10b}$$

where

$$\boldsymbol{p}_{tsc} \triangleq [p_{t1sc},\ p_{t2sc},\ \ldots,\ p_{t|\mathcal{G}_{tsc}|sc}]^\top \tag{11}$$

Constraint (10a) imposes power balance equation in which $\boldsymbol{d}_{tc} \in \mathbb{R}^{|\mathcal{V}|}$ represents nodal demand and the vector $\boldsymbol{B}_{tc}\theta_{tsc} \in \mathbb{R}^{|\mathcal{V}|}$ contains approximate values for active power exchanges between each vertex and the rest of the network. Additionally, constraint (10b) restricts the flow of power by the vector of line thermal limits $\boldsymbol{f}^{\max}_{tc} \in \mathbb{R}^{|\mathcal{E}_{tc}|}$, where $\boldsymbol{f}^{\text{shift}}_{tc}$ accounts for the effect of transformers and phase shifters.

Given the above three-part expression in (1) and constraints in (5)–(10), the Stochastic SCUC problem can be formulated as the optimization:

$$\text{minimize} \quad \text{(1a)+(1b)+(1c)} \tag{12a}$$
$$\text{subject to} \quad \text{(5)–(9)} \qquad \forall t \in \mathcal{T},\ \forall g \in \mathcal{G}_t \tag{12b}$$
$$\text{(10)} \qquad \forall t \in \mathcal{T} \tag{12c}$$

with respect to variables $\{x_{tg}\}$, $\{p_{tgsc}\}$, $\{p^{\text{contract}}_{tg}\}$, $\{r^+_{tg}\}$, $\{r^-_{tg}\}$, $\{w^+_{tg}\}$, and $\{w^-_{tg}\}$.

III. Convexification of SCUC Problem

In this section, we construct convex relaxations in order to efficiently tackle the SCUC problem (12). We employ conic relaxations combined with a set of valid inequalities which lead to a computationally-tractable convex formulation. To this end, we transition to a lifted space by introducing additional auxiliary variables each accounting for a quadratic monomial. We then formulate a SOCP relaxation based on the "perspective relaxation" in [40]. Finally, a strong SDP relaxation is formulated using additional variables and valid inequalities.

A. Lifted objective

To formulate convex relaxations we first lift the objective function (1) into a higher-dimensional space in which it is piecewise linear. This is done by introducing the variables

$$\{u_{tg}\}_{t\in\mathcal{T},\,g\in\mathcal{G}_t},\ \ \{h_{tgs_1s_2}\}_{t\in\mathcal{T},\,g\in\mathcal{G}_t,\,s_1\in\mathcal{S}_{t-1},\,s_2\in\mathcal{S}_t},$$
$$\{o_{tgsc}\}_{t\in\mathcal{T},\,g\in\mathcal{G}_t,\,s\in\mathcal{S}_t,\,c\in\mathcal{C}_{ts}}$$

representing the products

$$\{x_{(t-1)g}\,x_{tg}\},\ \ \{p_{(t-1)gs_10}\times p_{tgs_20}\},\ \ \{p^2_{tgsc}\} \tag{13}$$

respectively. Consider the following lifted objective function components:

$$\sum_{t\in\mathcal{T}}\gamma_t \sum_{g\in\mathcal{G}_t} \bar{\sigma}^{(1)}_{tg}(x_{tg}, u_{tg}, r^+_{tg}, r^-_{tg}, w^+_{tg}, w^-_{tg}) \tag{14a}$$
$$\sum_{t\in\mathcal{T}}\sum_{s\in\mathcal{S}_t}\sum_{c\in\mathcal{C}_{ts}} \psi_{tsc} \sum_{g\in\mathcal{G}_{tsc}} \bar{\sigma}^{(2)}_{tg}(p_{tgsc}, o_{tgsc}, p^{\text{contract}}_{tg}) \tag{14b}$$
$$\sum_{t\in\mathcal{T}}\gamma_t \sum_{s_1\in\mathcal{S}_{t-1}}\sum_{s_2\in\mathcal{S}_t}\phi_{ts_1s_2}\sum_{g\in\mathcal{G}_{ts_20}} \bar{\sigma}^{(3)}_{g}(o_{tgs_20}, o_{(t-1)gs_10}, h_{tgs_2s_1}) \tag{14c}$$

where for each $t \in \mathcal{T}$ and $g \in \mathcal{G}_t$

$$\bar{\sigma}^{(1)}_{tg}(x_{tg}, u_{tg}, r^+_{tg}, r^-_{tg}, w^+_{tg}, w^-_{tg}) \triangleq \zeta_{tg}\ x_{tg} \tag{15a}$$
$$+\ \zeta^{\uparrow}_{tg}\ (x_{tg} - u_{tg}) \tag{15b}$$
$$+\ \zeta^{\downarrow}_{tg}\ (x_{(t-1)g} - u_{tg}) \tag{15c}$$
$$+\ (\eta^+_{tg}\ r^+_{tg} + \eta^-_{tg}\ r^-_{tg}) \tag{15d}$$
$$+\ (\mu^+_{tg}\ w^+_{tg} + \mu^-_{tg}\ w^-_{tg}) \tag{15e}$$

encapsulates the lifted startup and shutdown costs and

$$\bar{\sigma}^{(2)}_{tg}(p_{tgsc}, o_{tgsc}, p^{\text{contract}}_{tg}) \triangleq \alpha^{\text{sqr}}_{tg}\ o_{tgsc} + \alpha^{\text{lin}}_{tg}\ p_{tgsc} + \tag{16a}$$
$$\frac{\beta^+_{tg}+\beta^-_{tg}}{2}\,|p_{tgsc} - p^{\text{contract}}_{tg}| + \frac{\beta^+_{tg}-\beta^-_{tg}}{2}(p_{tgsc} - p^{\text{contract}}_{tg}). \tag{16b}$$

represents the lifted quadratic cost function. Additionally, for each $g \in \mathcal{G}$,

$$\bar{\sigma}^{(3)}_{g}(o_{tgs_20}, o_{(t-1)gs_10}, h_{tgs_1s_2}) \triangleq$$
$$\kappa_g \times (o_{tgs_20} + o_{(t-1)gs_10} - 2h_{tgs_1s_2}) \tag{17}$$

is the lifted "wear and tear" cost.

B. LP and perspective relaxations

For every $t \in \mathcal{T}$ and $g \in \mathcal{G}_t$, the relation between the auxiliary variables $\{u_{tg}\}$ and their corresponding monomials can be enforced using the following valid inequalities:

$$\max\{0,\ x_{(t-1)g} + x_{tg} - 1\} \le u_{tg} \le \min\{x_{(t-1)g}, x_{tg}\} \tag{18}$$

The role of (18) is to ensure that the lifted costs (14a) is equivalent to the original costs (1a). Through simple enumeration of the set $(x_{g(t-1)}, x_{gt}) \in \{0,1\}^2$, it can be observed that

$$\text{(5)} \wedge \text{(18)} \quad \Rightarrow \quad u_{tg} = x_{tg}x_{(t-1)g}$$

0885-8950 (c) 2021 IEEE. Personal use is permitted, but republication/redistribution requires IEEE permission. See http://www.ieee.org/publications_standards/publications/rights/index.html for more information.
Authorized licensed use limited to: University of Texas at Arlington. Downloaded on April 01,2021 at 15:39:46 UTC from IEEE Xplore. Restrictions apply.

This article has been accepted for publication in a future issue of this journal, but has not been fully edited. Content may change prior to final publication. Citation information: DOI 10.1109/TPWRS.2021.3062203, IEEE Transactions on Power Systems

for every $t \in \mathcal{T}$ and $g \in \mathcal{G}_t$.

Lifting the first part of the objective and the transformation of $x_{gt} \in \{0,1\}$ to $0 \leq x_{tg} \leq 1$, results in the following LP relaxation of SCUC [41]–[43]:

$$\begin{aligned}
&\text{minimize} && \text{(14a)+(1b)+(1c)} && && (19a)\\
&\text{subject to} && 0 \leq x_{tg} \leq 1 && \forall t \in \mathcal{T},\ \forall g \in \mathcal{G}_t && (19b)\\
& && (6)-(9),\ (18) && \forall t \in \mathcal{T},\ \forall g \in \mathcal{G}_t && (19c)\\
& && (10) && \forall t \in \mathcal{T} && (19d)
\end{aligned}$$

As shown in [40], the performance of this approach can be significantly improved by lifting (1b) to (14b), and relaxing $o_{tgsc} = p^2_{tgsc}$ to the SOCP and McCormick constraint

$$o_{tgsc}\, x_{tg} \geq p^2_{tgsc}, \quad o_{tgsc} \geq 0 \qquad \forall s \in \mathcal{S}_t,\ \forall c \in \mathcal{C}_{ts} \quad (20a)$$

$$o_{tgsc} + \underline{p}_g\, \bar{p}_g\, x_{tg} \leq (\underline{p}_g + \bar{p}_g) p_{tgsc} \qquad \forall s \in \mathcal{S}_t,\ \forall c \in \mathcal{C}_{ts} \quad (20b)$$

which results in the following perspective relaxation:

$$\begin{aligned}
&\text{minimize} && \text{(14a)+(14b)+(1c)} && && (21a)\\
&\text{subject to} && 0 \leq x_{tg} \leq 1 && \forall t \in \mathcal{T},\ \forall g \in \mathcal{G}_t && (21b)\\
& && (6)-(9),\ (18),\ (20) && \forall t \in \mathcal{T},\ \forall g \in \mathcal{G}_t && (21c)\\
& && (10) && \forall t \in \mathcal{T} && (21d)
\end{aligned}$$

In the remainder of this section, we will construct an SDP relaxation as an alternative to (21).

C. SDP relaxation

To forge a stronger relaxation, consider the new variables

$$\{z_{tgs}\}_{t\in\mathcal{T},\, g\in\mathcal{G}_t,\, s\in\mathcal{S}_t}, \qquad \{y_{tgs}\}_{t\in\mathcal{T},\, g\in\mathcal{G}_t,\, s\in\mathcal{S}_t}$$

representing monomials $\{p_{(t-1)gs0}x_{tg}\}$ and $\{p_{tgs0}x_{(t-1)g}\}$, respectively. In place of (19b), we impose a collection of conic and linear inequalities (22), resulting in the following SDP relaxation of SCUC:

$$\begin{aligned}
&\text{minimize} && \text{(14a)+(14b)+(14c)} && && (23a)\\
&\text{subject to} && (22) && \forall t \in \mathcal{T},\ \forall g \in \mathcal{G}_t && (23b)\\
& && (6)-(9),\ (18),\ (20) && \forall t \in \mathcal{T},\ \forall g \in \mathcal{G}_t && (23c)\\
& && (10) && \forall t \in \mathcal{T} && (23d)
\end{aligned}$$

The matrix inequality (22a) is a surrogate for:

$$\begin{bmatrix}
x_{(t-1)g} & * & * & * & *\\
u_{tg} & x_{tg} & * & * & *\\
u_{tg} & u_{tg} & u_{tg} & * & *\\
p_{(t-1)gs_10} & z_{tgs_1} & z_{tgs_1} & o_{(t-1)gs_10} & *\\
y_{tgs_1} & p_{tgs_20} & y_{tgs_1} & h_{tgs_1s_2} & o_{tgs_20}
\end{bmatrix} =$$

$$\begin{bmatrix}
x_{(t-1)g}\\ x_{tg}\\ u_{tg}\\ p_{(t-1)gs_10}\\ p_{tgs_10}
\end{bmatrix}
\begin{bmatrix} x_{(t-1)g} & x_{tg} & u_{tg} & p_{(t-1)gs_10} & p_{tgs_10} \end{bmatrix} \quad (24)$$

If equality holds at optimality, then the above relations are satisfied and the relaxation is regarded as exact. To further strengthen the proposed relaxation, we incorporate the Reformulation-Linearization Technique (RLT) technique [44]. Linear inequalities (22b) – (22e) are derived from (6). Lastly, inequalities (22g) – (22i) are immediate consequences of (5) and (6).

The variables that appear in (22) are tightly correlated and this is the primary motivation behind the proposed valid inequalities. In Section (V), we will demonstrate the effect of these additional inequalities on the quality of relaxation and their ability to obtain feasible points.

IV. Feasible Point Recovery

Let $\{x^{\text{rlx}}_{tg}\}_{t\in\mathcal{T},\, g\in\mathcal{G}_t}$ denote the resulting schedule from a convex relaxation of SCUC. For large-scale problems, convex relaxations can fail to satisfy the integrality constraint (5). In this section, we propose a heuristic to infer a feasible point $\{\hat{x}_{tg} \in \{0,1\}\}_{t\in\mathcal{T},\, g\in\mathcal{G}_t}$. To this end, the main challenge is to ensure that the minimum up and minimum down constraints (7a) and (7b) are satisfied, which is not possible by simply rounding x^{rlx}_{tg} values. To tackle this issue we adopt the following procedure.

Feasible Point Recovery:

1) For every $t \in \mathcal{T}$ and $g \in \mathcal{G}_t$ do $x^{\text{rnd}}_{tg} \leftarrow \text{round}\{0.4 + x^{\text{rlx}}_{tg}\}$.

2) For every $g \in \cup_{t\in\mathcal{T}}\mathcal{G}_t$,

(a) Solve the following linear program

$$\begin{aligned}
&\text{minimize} && \sum_{t\in\mathcal{T}} |x_{tg} - x^{\text{rnd}}_{tg}| && && (25a)\\
&\text{subject to} && x_{tg} = 0 && \text{if} \quad g \notin \mathcal{G}_t && (25b)\\
& && 0 \leq x_{tg} \leq 1 && \text{if} \quad g \in \mathcal{G}_t && (25c)\\
& && x_{tg} \geq x_{\tau g} - x_{(\tau-1)g} && \forall t \in \mathcal{T},\ \forall \tau \in \{t - m^{\uparrow}_g + 1, \ldots, t\} && (25d)\\
& && 1 - x_{tg} \geq x_{(\tau-1)g} - x_{\tau g} && \forall t \in \mathcal{T},\ \forall \tau \in \{t - m^{\downarrow}_g + 1, \ldots, t\} && (25e)
\end{aligned}$$

and denote the resulting solution as $\{\hat{x}_{tg}\}_{t\in\mathcal{T}}$.

(b) For $t = 1, \ldots, |\mathcal{T}|$ do

$$a^{\uparrow}_{tg} \leftarrow \max\{\hat{x}_{\tau g} - \hat{x}_{(\tau-1)g} \mid \forall \tau \in \{t - m^{\uparrow}_g + 1, \ldots, t\}\}, \quad (26a)$$

$$a^{\downarrow}_{tg} \leftarrow \max\{\hat{x}_{(\tau-1)g} - \hat{x}_{\tau g} \mid \forall \tau \in \{t - m^{\downarrow}_g + 1, \ldots, t\}\}, \quad (26b)$$

$$\text{if} \quad a^{\uparrow}_{tg} = 0 \ \wedge\ a^{\downarrow}_{tg} = 0 \quad \text{then} \quad \hat{x}_{tg} \leftarrow x^{\text{rnd}}_{tg}, \quad (26c)$$

$$\text{if} \quad a^{\uparrow}_{tg} = 0 \ \wedge\ a^{\downarrow}_{tg} = 1 \quad \text{then} \quad \hat{x}_{tg} \leftarrow 0, \quad (26d)$$

$$\text{if} \quad a^{\uparrow}_{tg} = 1 \ \wedge\ a^{\downarrow}_{tg} = 0 \quad \text{then} \quad \hat{x}_{tg} \leftarrow 1, \quad (26e)$$

$$\text{if} \quad a^{\uparrow}_{tg} = 1 \ \wedge\ a^{\downarrow}_{tg} = 1 \quad \text{then declare failure.} \quad (26f)$$

3) Declare $\{\hat{x}_{tg}\}_{t\in\mathcal{T},\, g\in\mathcal{G}_t}$ as the recovered schedule and solve the convex optimization

$$\begin{aligned}
&\text{minimize} && \text{(1a)+(1b)+(1c)} && && (27a)\\
&\text{subject to} && x_{tg} = \hat{x}_{tg} && \forall t \in \mathcal{T},\ \ \forall g \in \mathcal{G}_t && (27b)\\
& && (6)-(9) && \forall t \in \mathcal{T},\ \ \forall g \in \mathcal{G}_t && (27c)\\
& && (10) && \forall t \in \mathcal{T} && (27d)
\end{aligned}$$

to obtain a feasible point:

$$\{\hat{x}_{tg},\ \hat{p}^{\text{contract}}_{tg},\ \hat{r}^{+}_{tg},\ \hat{r}^{-}_{tg},\ \hat{w}^{+}_{tg},\ \hat{w}^{-}_{tg} \in \mathbb{R}\}_{t\in\mathcal{T},\, g\in\mathcal{G}_t}$$

$$\{\hat{p}_{tgsc}\}_{t\in\mathcal{T},\, g\in\mathcal{G}_t,\, s\in\mathcal{S}_t,\, c\in\mathcal{C}_{ts}}, \quad \{\hat{\boldsymbol{\theta}}_{tsc} \in \mathbb{R}^{|\mathcal{V}|}\}_{t\in\mathcal{T},\, s\in\mathcal{S}_t,\, c\in\mathcal{C}_{ts}}.$$

In case of infeasibility, declare failure.

0885-8950 (c) 2021 IEEE. Personal use is permitted, but republication/redistribution requires IEEE permission. See http://www.ieee.org/publications_standards/publications/rights/index.html for more information.
Authorized licensed use limited to: University of Texas at Arlington. Downloaded on April 01,2021 at 15:39:46 UTC from IEEE Xplore. Restrictions apply.

This article has been accepted for publication in a future issue of this journal, but has not been fully edited. Content may change prior to final publication. Citation information: DOI 10.1109/TPWRS.2021.3062203, IEEE Transactions on Power Systems

$$\begin{bmatrix} x_{(t-1)g} & * & * & * & * \\ u_{tg} & x_{tg} & * & * & * \\ u_{tg} & u_{tg} & u_{tg} & * & * \\ p_{(t-1)gs_10} & z_{tgs_1} & z_{tgs_1} & o_{(t-1)gs_10} & * \\ y_{tgs_1} & p_{tgs_20} & y_{tgs_1} & h_{tgs_1s_2} & o_{tgs_20} \end{bmatrix} \succeq 0 \qquad \forall s_1 \in \mathcal{S}_{t-1},\ \forall s_2 \in \mathcal{S}_t \tag{22a}$$

$$\underline{p}_g \left(p_{tgs_10} + p_{tgs_20}\right) \ \leq \ h_{tgs_1s_2} + \underline{p}_g^2\, u_{tg} \qquad \forall s_1 \in \mathcal{S}_{t-1},\ \forall s_2 \in \mathcal{S}_t \tag{22b}$$

$$\bar{p}_g \left(p_{tgs_10} + p_{tgs_20}\right) \ \leq \ h_{tgs_1s_2} + \bar{p}_g^2\, u_{tg} \qquad \forall s_1 \in \mathcal{S}_{t-1},\ \forall s_2 \in \mathcal{S}_t \tag{22c}$$

$$h_{tgs_1s_2} + \underline{p}_g \bar{p}_g\, u_{tg} \ \leq \ \bar{p}_g\, y_{tgs_1} + \underline{p}_g\, z_{tgs_1} \qquad \forall s_1 \in \mathcal{S}_{t-1},\ \forall s_2 \in \mathcal{S}_t \tag{22d}$$

$$h_{tgs_1s_2} + \underline{p}_g \bar{p}_g\, u_{tg} \ \leq \ \underline{p}_g\, y_{tgs_1} + \bar{p}_g\, z_{tgs_1} \qquad \forall s_1 \in \mathcal{S}_{t-1},\ \forall s_2 \in \mathcal{S}_t \tag{22e}$$

$$\underline{p}_g\, u_{tg} \ \leq \ y_{tgs_1} \ \leq \ \bar{p}_g\, u_{tg} \qquad \forall s \in \mathcal{S}_t \tag{22f}$$

$$\underline{p}_g\, u_{tg} \ \leq \ z_{tgs_1} \ \leq \ \bar{p}_g\, u_{tg} \qquad \forall s \in \mathcal{S}_t \tag{22g}$$

$$\bar{p}_g \left(u_{tg} - x_{tg}\right) \ \leq \ y_{tgs_1} - p_{tgs0} \ \leq \ \underline{p}_g \left(u_{tg} - x_{tg}\right) \qquad \forall s \in \mathcal{S}_t \tag{22h}$$

$$\bar{p}_g \left(u_{tg} - x_{(t-1)g}\right) \ \leq \ z_{tgs_1} - p_{(t-1)gs0} \ \leq \ \underline{p}_g \left(u_{tg} - x_{(t-1)g}\right) \qquad \forall s \in \mathcal{S}_t \tag{22i}$$

As we will demonstrate in Section (V), this heuristic is able to obtain good quality feasible points for challenging instances of SCUC. We use the following measure to evaluate the quality of the resulting feasible points:

$$\text{Optimality Gap } \% = 100 \times \frac{\hat{\sigma} - \sigma^{\text{rlx}}}{\hat{\sigma}} \tag{28}$$

where σ^{rlx} and $\hat{\sigma}$ are the optimal objective values for convex relaxation and the recovery problem (27), respectively.

V. Experiments

In this section, we demonstrate the performance of the proposed convex relaxation on a wide range of challenging SCUC problems. Simulations are performed on a 64-bit computer with an Intel 3.0 GHz, 12-core CPU and 256 GB RAM using MATLAB 2019a. The solver MOSEK v8.0.0.60 [45] is used for convex optimization through CVX v2.1 [46], [47]. SCUC problems are formulated using the MATPOWER Optimal Scheduling Tool (MOST) v1.0.2 [48]. For comparison, CPLEX v12.9.0.0 [49] and GUROBI v9.0 are used for mixed-integer programming through MOST. We would like to emphasis that CPLEX and GUROBI may exhibit far better performance on the same problem, if applied differently. System operators and utility companies may leverage stronger MILP formulations and valid inequalities in order to strengthen the performance of SCUC.

A. Data

Transmission Network Data: We use IEEE and Pan European Grid Advanced Simulation and State Estimation (PEGASE) benchmark grids from MATPOWER [48]. Certain modifications are made to the following parts of the data in order to make the resulting SCUC problems feasible and sufficiently challenging:

- $\boldsymbol{f}_{tc}^{\max}$: Line thermal limits specified in MATPOWER data files were used without modifications. Source data on line flow limits are specified in the documentation of MATPOWER data files [48].
- $\boldsymbol{d}_{tc}$: With no loss of generality, we assume that all loads are deterministic and we do not consider the contingency of loads. In all of the simulations, load variations throughout the day, follow the vector:

  $$\begin{aligned}\boldsymbol{\pi}^{\text{gen}} \triangleq \nu^{\text{gen}} \times [&0.684,\ 0.645,\ 0.620,\ 0.604,\ 0.606,\ 0.627 \\ &0.677,\ 0.694,\ 0.730,\ 0.808,\ 0.893,\ 0.922 \\ &0.946,\ 0.952,\ 0.972,\ 0.999,\ 1.000,\ 0.964 \\ &0.961,\ 0.927,\ 0.927,\ 0.909,\ 0.765,\ 0.764]\end{aligned}$$

  where $\nu^{\text{gen}} = 0.9$ for case New England 39-bus system and $\nu^{\text{gen}} = 0.5$ for all of the other benchmark cases. In other words, for every $t \in \mathcal{T}$ and $c \in \cup_{s \in \mathcal{S}_t} \mathcal{C}_{ts}$ we have $\boldsymbol{d}_{tc} = \pi_t^{\text{gen}}\, \boldsymbol{d}$, where $\boldsymbol{d}$ is the vector of nodal demand from MATPOWER.

In addition to the above modifications, we have added wind generators to certain buses and altered generator costs due to the absence of fixed, quadratic, reserve and load-following costs in MATPOWER data. These changes are detailed next.

Deterministic Generator Cost Data:

- α_{tg}^{sqr}, α_{tg}^{lin}, ζ_{tg}, $\zeta_{tg}^{\uparrow}$, $\zeta_{tg}^{\downarrow}$: These cost coefficients are randomly chosen based on uniform distributions within $\pm 20\%$ of mean values \$0.0025/(MW.h)^2, \$20/(MW.h), \$500/h, \$5000/h, and \$500/h, respectively following [50], [51] .
- η_{tg}^{+}, η_{tg}^{-}, μ_{tg}^{+}, μ_{tg}^{-}: Reserve cost coefficients are selected as $\eta_{tg}^{+} = \eta_{tg}^{-} = 5.0\, \alpha_{tg}^{\text{lin}}$ and $\mu_{tg}^{+} = \mu_{tg}^{-} = 0.2\, \alpha_{tg}^{\text{lin}}$.
- β_{tg}^{+}, β_{tg}^{-}: Active power re-dispatch cost coefficients are selected as $\beta_{tg}^{+} = \beta_{tg}^{-} = 0.2\, \alpha_{tg}^{\text{lin}}$.
- κ_g: Ramp "wear and tear" cost coefficients are selected as $\kappa_g = 500 \alpha_{tg}^{\text{sqr}}$.

Deterministic Generator Limits:

- $\underline{p}_g$: Minimum active power is selected as $\underline{p}_g = 0$.
- $m_g^{\uparrow}$, $m_g^{\downarrow}$: A quarter of the generators are randomly selected with $m_g^{\uparrow} = m_g^{\downarrow} = 1$ to act as fast-start units that

0885-8950 (c) 2021 IEEE. Personal use is permitted, but republication/redistribution requires IEEE permission. See http://www.ieee.org/publications_standards/publications/rights/index.html for more information.
Authorized licensed use limited to: University of Texas at Arlington. Downloaded on April 01,2021 at 15:39:46 UTC from IEEE Xplore. Restrictions apply.

This article has been accepted for publication in a future issue of this journal, but has not been fully edited. Content may change prior to final publication. Citation information: DOI 10.1109/TPWRS.2021.3062203, IEEE Transactions on Power Systems

have the capacity to ramp-up quickly in order to support generation shortfalls. For the remaining generators

$$m_g^{\uparrow} = \min\left\{\tilde{m}_g^{\uparrow} + 1,\ \lfloor |\mathcal{T}|/2 \rfloor\right\}$$
$$m_g^{\downarrow} = \min\left\{\tilde{m}_g^{\downarrow} + 1,\ \lfloor |\mathcal{T}|/2 \rfloor\right\}$$

where each $\tilde{m}_g^{\uparrow}$ and $\tilde{m}_g^{\downarrow}$ has Poisson distribution with parameter 4.

- The initial state of each generator is uniformly chosen from the set of integers $\{k \in \mathbb{Z} \,|\, -5 \leq k \leq 5\} \setminus \{0\}$ with negative and positive numbers, respectively, indicating the number of uptime and downtime periods at $t = 0$.
- $\bar{w}_{tg}$, $\underline{w}_{tg}$, $\bar{r}_{tg}$, $\underline{r}_{tg}$, $\bar{\Delta}_g$, $\underline{\Delta}_g$: Following [39], ramp limits are selected as $\bar{w}_{tg} = \underline{w}_{tg} = 0.3\bar{p}$ and $\bar{r}_{tg} = \underline{r}_{tg} = \bar{\Delta}_g = \underline{\Delta}_g = 0.1\bar{p}$.

Wind Generator Data: Data on wind generators and hourly wind profile are obtained from the SW Minnesota wind power plant [52]. Let $|\mathcal{G}|$ indicate the total number of deterministic generators. We consider $\text{round}\{|\mathcal{G}|/3\}$ wind generators, each located at a randomly chosen bus. We consider 5 wind scenarios representing 100%, 80%, 60% 40%, and %20 wind generation, with initial probabilities

$$\Phi_1 = \begin{bmatrix} 0.11 & 0.48 & 0.17 & 0.17 & 0.07 \end{bmatrix}^{\top} \quad (29)$$

respectively. Additionally, for every $t \in \mathcal{T} \setminus \{1\}$ the transition probability matrix is set to

$$\Phi_t = \begin{bmatrix} 0.7858 & 0.2001 & 0.0109 & 0.0032 & 0 \\ 0.1022 & 0.6215 & 0.2381 & 0.0371 & 0.0012 \\ 0.0154 & 0.3184 & 0.5042 & 0.1439 & 0.0181 \\ 0.0022 & 0.0356 & 0.2488 & 0.5435 & 0.1698 \\ 0 & 0.0004 & 0.0073 & 0.0543 & 0.9379 \end{bmatrix} \quad (30)$$

The scenario transition probabilities $\phi_{ts_1s_2}$ are obtained from the SW Minnesota wind power plant [52]. The coefficients of (29) – (30) is used to weight ramp "wear and tear" cost in (1c).

- α_{tg}^{lin}, ζ_{tg}, $\zeta_{tg}^{\uparrow}$, $\zeta_{tg}^{\downarrow}$: Wind energy cost coefficients are selected as $\alpha_{tg}^{\text{lin}} =$ \$20/(MW.h), $\zeta_{tg} =$ \$20/h, and $\zeta_{tg}^{\uparrow} = \zeta_{tg}^{\downarrow} =$ \$0/h.
- Wind generator output is given by the product of the maximum wind generator output from MATPOWER [1] and the ratios

$$\boldsymbol{\pi}^{\text{wind}} \triangleq [\,0.72,\ 0.61,\ 0.35,\ 0.28,\ 0.15,\ 0.39$$
$$0.25,\ 0.35,\ 0.29,\ 0.57,\ 0.49,\ 0.37$$
$$0.52,\ 0.34,\ 0.42,\ 0.41,\ 0.63,\ 0.42$$
$$0.29,\ 0.53,\ 0.79,\ 0.83,\ 0.81,\ 0.87\,]$$

Contingencies: We consider N-1 contingency analysis in this study. 3 generators and 3 lines are randomly selected each representing a contingency with probability $1/60$.

- ψ_{tsc}: Base scenario conditional probabilities are selected as $\psi_{ts0} = 0.1/|\mathcal{C}|$ for every $s \in \mathcal{S}$. Additionally, for every $c \in \mathcal{C}$ post-contingency probabilities are given by:

$$\begin{bmatrix} \psi_{t1c} \\ \psi_{t2c} \\ \vdots \\ \psi_{t|\mathcal{S}|c} \end{bmatrix} = \frac{1}{|\mathcal{C}|} \times \Phi_t \begin{bmatrix} \psi_{(t-1)10} \\ \psi_{(t-1)20} \\ \vdots \\ \psi_{(t-1)|\mathcal{S}|0} \end{bmatrix} \quad (31)$$

- γ_t: Lastly, the probability of making it to period t without branching off the central path in a contingency is given by:

$$\gamma_t = \sum_{s \in \mathcal{S}_t} \psi_{(t-1)s0} \ = \sum_{s \in \mathcal{S}_t,\ c \in \mathcal{C}_{ts}} \psi_{tsc} \leq 1, \text{ for } t \geq 1 \quad (32)$$

B. Evaluation of Lower Bound

In order to evaluate the performance of our proposed SDP relaxation, we consider 5 benchmark grids based on IEEE and PEGASE modified data. Each benchmark grid is simulated in 4 realizations producing 20 test cases. The planning horizon is divided into 24 hourly intervals, 6 stochastic wind scenarios and 6 independent contingencies. The largest grid considered is PEGASE 2869 benchmark grid with 2,869 buses (vertices) and 510 generating units. For the largest benchmark, the model has 12,240 binary decision variables and 1,830,560 continuous variables. Table I presents details on the benchmark grids.

Table II reports performance of SDP relaxation compared to CPLEX and GUROBI numerical solvers and also perspective and LP relaxation methods. Performance is compared in terms of: i) convex lower bound (LB) on the optimal cost, ii) cost of the recovered feasible solution, iii) optimality gap and iv) computation time $t(s)$. In all experiments performed using SDP relaxation, we successfully infer a feasible point using heuristics presented in Section (IV). The reported gaps in Table II show that SDP relaxation achieves average of 0.05% and does not exceed 0.36% optimality gap for all the test cases. This is better than average gap reported by both perspective and LP relaxations. Computation time reported by SDP relaxation averages at 35 mins. 35 sec.

C. Solution Quality

Figures 1a and 2a emphasize disparities in the number of inexact binaries generated by SDP, perspective and LP methods of relaxation for large test cases such as PEGASE 1354 and PEGASE 2869. As shown in Figures 1a and 2a, SDP relaxation generates fewer inexact binaries between '0' and '1' as compared to perspective and LP relaxations. Figures 1b, 1c, 2b and 2c shows that perspective and LP relaxations report higher number of inexact binaries. Poor solution quality negatively impacts ability of the proposed heuristic to infer a feasible point resulting in failed recoveries. Table II shows failed recoveries in experiments 15, 17 and 19 using perspective relaxation and experiments 14, 15 and 19 using LP relaxation due to poor solution quality. As seen from the table, all experiments using SDP relaxation produced feasible solutions because of fewer inexact binaries.

0885-8950 (c) 2021 IEEE. Personal use is permitted, but republication/redistribution requires IEEE permission. See http://www.ieee.org/publications_standards/publications/rights/index.html for more information.
Authorized licensed use limited to: University of Texas at Arlington. Downloaded on April 01,2021 at 15:39:46 UTC from IEEE Xplore. Restrictions apply.

This article has been accepted for publication in a future issue of this journal, but has not been fully edited. Content may change prior to final publication. Citation information: DOI 10.1109/TPWRS.2021.3062203, IEEE Transactions on Power Systems

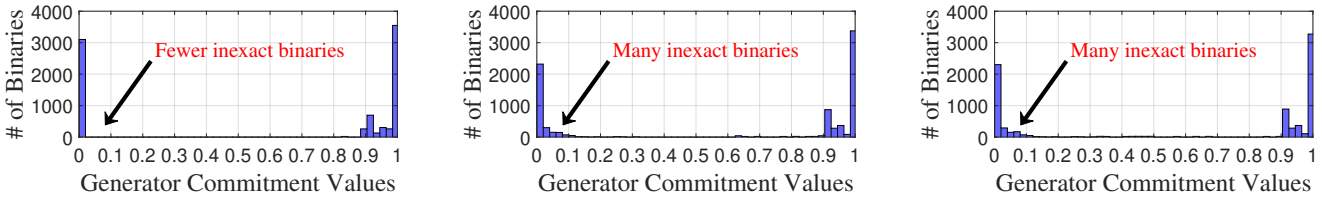

(a) SDP relaxation (b) Perspective relaxation (c) LP relaxation

Fig. 1: Distribution of Binary variables for PEGASE 1354 (Experiment 14) in 24-hour horizon scheduling

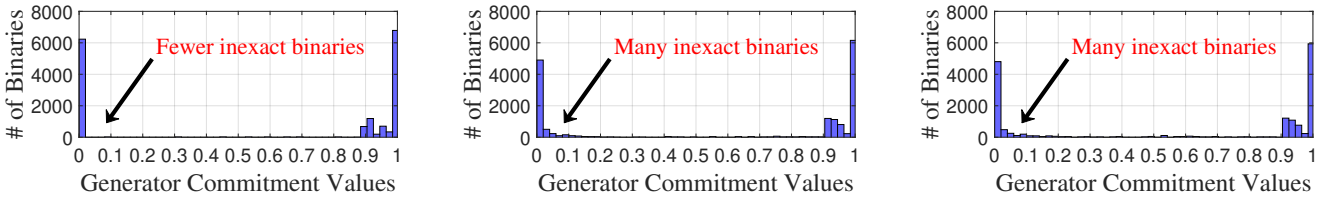

(a) SDP relaxation (b) Perspective relaxation (c) LP relaxation

Fig. 2: Distribution of Binary variables for PEGASE 2869 (Experiment 17) in 24-hour horizon scheduling

TABLE I: Experiments for 24-hour horizon scheduling of benchmark systems

Experiment	Test Cases	# of Generators	# of Binaries	# of Continuous variables
1	New England 39-bus	10	240	67,750
2	New England 39-bus	10	240	67,750
3	New England 39-bus	10	240	67,750
4	New England 39-bus	10	240	67,750
5	IEEE 118	54	1,296	191,664
6	IEEE 118	54	1,296	191,664
7	IEEE 118	54	1,296	191,664
8	IEEE 118	54	1,296	191,664
9	IEEE 300	69	1,656	247,664
10	IEEE 300	69	1,656	247,664
11	IEEE 300	69	1,656	247,664
12	IEEE 300	69	1,656	247,664
13	PEGASE 1354	260	6,240	928,925
14	PEGASE 1354	260	6,240	928,925
15	PEGASE 1354	260	6,240	928,925
16	PEGASE 1354	260	6,240	928,925
17	PEGASE 2869	510	12,240	1,830,560
18	PEGASE 2869	510	12,240	1,830,560
19	PEGASE 2869	510	12,240	1,830,560
20	PEGASE 2869	510	12,240	1,830,560

D. Hourly Profile

Fig. 3 depicts the 24-hr profile of selected generators and transmission lines in SCUC experiment 1 on New-England 39 bus benchmark system. The data and the resulting commitment keys for this particular experiment are given by Tables III and IV. In the figure, Gen. #5 and line #38 are shown in pre and post-contingency states, and Gen. #2 in post-contingency state. Post-contingency #1 represents outage of Gen. #3 while post-contingency #6 represents loss of line #35. In Fig. 3, hourly profile is divided into 3 scenarios with probability assigned to transition from one scenario to the other. Notice that during on-peak hours 12PM – 10PM, Gen. #2 drives up to maximum output power in order to supply peak load in pre and post-contingency states. Likewise, Gen. #5 sees a significant upward climb in output power in post-contingency #1 in order to compensate for outage to Gen. #3. This presents stress on the network which is discussed next and illustrated by 4.

As seen in Fig. 3, line #38 shows signs of congestion in post-contingency #6 due to loss of line #35 during on-peak hours. Of significance, line flows in post-contingency state is almost three times higher than line flows before contingency occurred. The impact of high wind penetration on generator and line congestion is seen between 9PM – 1AM. Between 9PM – 1AM, wind penetration is at its highest point coinciding with congested generators and line flows. This results in the noticeable decline in line flows and power generation seen between 9PM – 1AM in Fig. 3.

E. Network Congestion

Fig. 4 shows the contrast in network congestion between pre and post-contingency states of New England 39-bus benchmark grid. As seen in Fig. 4a, all 46 transmission lines operate within thermal limits with some lines transmitting more power than others as indicated by varying thickness of lines in the figure. Directional arrows are used to show the flow of power throughout the grid network.

In post-contingency state #6 depicted in Fig. 4b, we observe network congestion during peak hours of the day. The loss of line #35 in this contingency results in congestion on transmission line connecting bus 23 to 24 at severe levels attributed to increased flow of power in order to supply peak load at bus 24. The contingency also results in reversal of flow on line connecting bus 16 to 21 and line connecting bus 16 to 24. Power flow is increased on neighboring lines in attempts to compensate for loss of line #35 as observed in line from bus 22 to bus 23, as well as bus 32 to bus 10 to mention a few.

We observe that line contingencies make the SCUC problem more challenging since power flow is redirected to compensate for the sudden loss of a line or a generator. Since line flows

0885-8950 (c) 2021 IEEE. Personal use is permitted, but republication/redistribution requires IEEE permission. See http://www.ieee.org/publications_standards/publications/rights/index.html for more information.
Authorized licensed use limited to: University of Texas at Arlington. Downloaded on April 01,2021 at 15:39:46 UTC from IEEE Xplore. Restrictions apply.

This article has been accepted for publication in a future issue of this journal, but has not been fully edited. Content may change prior to final publication. Citation information: DOI 10.1109/TPWRS.2021.3062203, IEEE Transactions on Power Systems

TABLE II: The performance of SDP relaxation algorithm for 24-hour horizon scheduling of benchmark systems (4 realizations in each benchmark system)

Exp.	Test Case	CPLEX			GUROBI			SDP Relaxation					Perspective Relaxation					LP Relaxation				
		Feasible	GAP (%)	t(s)	Feasible	GAP (%)	t(s)	LB	Feasible	GAP (%)	Determined Binaries (%)	t(s)	LB	Feasible	GAP (%)	Determined Binaries (%)	t(s)	LB	Feasible	GAP (%)	Determined Binaries (%)	t(s)
1	NE 39 bus	-2.621e+6	0.00	94.26	-2.621e+6	0.00	442.81	-2.621e+6	-2.621e+6	0.002	100	42.7	-2.623e+6	-2.620e+6	0.076	92.92	7.55	-2.627e+6	-2.620e+6	0.153	92.92	7.05
2	NE 39 bus	-1.337e+6	0.00	119.59	-1.337e+6	0.00	473.75	-1.337e+6	-1.337e+6	0.008	99.58	39.78	-1.339e+6	-1.337e+6	0.147	96.67	7.05	-1.340e+6	-1.337e+6	0.055	96.67	6.06
3	NE 39 bus	-1.867e+6	0.15	81.94	-1.867e+6	0.00	247.77	-1.867e+6	-1.867e+6	0.020	98.75	30.7	-1.871e+6	-1.867e+6	0.174	85	7.53	-1.873e+6	-1.867e+6	0.123	85	6.88
4	NE 39 bus	-2.149e+6	0.08	163.27	-2.149e+6	0.00	588.68	-2.150e+6	-2.149e+6	0.065	97.92	33.67	-2.152e+6	-2.149e+6	0.064	90.42	8.16	-2.159e+6	-2.149e+6	0.331	90.42	6.11
5	IEEE 118	–	–	3,600†	–	–	3,600†	-5.592e+5	-5.592e+5	6.496e-4	100	721.7	-5.592e+5	-5.592e+5	3.493e-5	100	40.8	-5.621e+5	-5.592e+5	0.518	100	38.34
6	IEEE 118	–	–	3,600†	–	–	3,600†	-8.022e+5	-8.022e+5	4.642e-4	100	879.89	-8.022e+5	-8.022e+5	4.053e-6	100	46.56	-8.062e+5	-8.022e+5	0.491	100	40.19
7	IEEE 118	–	–	3,600†	–	–	3,600†	-9.297e+5	-9.297e+5	5.577e-5	100	789.39	-9.297e+5	-9.297e+5	3.270e-6	100	38.17	-9.304e+5	-9.297e+5	0.073	100	39.94
8	IEEE 118	–	–	3,600†	–	–	3,600†	-3.064e+5	-3.064e+5	2.006e-4	100	783.75	-3.064e+5	-3.064e+5	6.499e-4	100	46.38	-3.145e+5	-3.064e+5	2.646	100	41.69
9	IEEE 300	–	–	3,600†	–	–	3,600†	-9.214e+6	-9.208e+6	0.069	93.78	1,128.7	-9.215e+6	-9.207e+6	0.016	93.12	67.89	-9.229e+6	-9.207e+6	0.145	93.12	51.25
10	IEEE 300	–	–	3,600†	–	–	3,600†	-3.498e+6	-3.498e+6	2.903e-4	100	1,071.2	-3.501e+6	-3.497e+6	0.070	98.25	52.23	-3.516e+6	-3.497e+6	0.446	98.25	47.7
11	IEEE 300	–	–	3,600†	–	–	3,600†	-6.558e+6	-6.558e+6	1.012e-4	100	1,279.2	-6.560e+6	-6.555e+6	0.028	96.01	47.59	-6.574e+6	-6.555e+6	0.220	96.01	39.88
12	IEEE 300	–	–	3,600†	–	–	3,600†	-8.045e+6	-8.040e+6	0.057	95.59	1,291.5	-8.048e+6	-8.038e+6	0.032	93.06	56.06	-8.060e+6	-8.038e+6	0.158	93.06	50.77
13	PEGASE 1354	–	–	3,600†	–	–	3,600†	-3.463e+7	-3.459e+7	0.129	97.76	6,444.9	-3.470e+7	-9.231e+6	0.194	91.55	364.22	-3.488e+7	-9.886e+6	0.512	91.55	298.52
14	PEGASE 1354	–	–	3,600†	–	–	3,600†	-3.441e+7	-3.440e+7	0.003	99.63	9,278.9	-3.447e+7	-9.828e+6	0.184	94.38	400.83	-3.457e+7	–	0.303	94.38	301.88
15	PEGASE 1354	–	–	3,600†	–	–	3,600†	-2.827e+7	-2.826e+7	0.036	97.45	5,496.4	-2.834e+7	–	0.238	91.43	347.55	-2.851e+7	–	0.604	91.43	279.64
16	PEGASE 1354	–	–	3,600†	–	–	3,600†	-3.837e+7	-3.823e+7	0.354	96.39	6,203.6	-3.849e+7	-1.282e+7	0.323	90.79	368.33	-3.864e+7	-1.363e+7	0.374	90.79	321.2
17	PEGASE 2869	–	–	3,600†	–	–	3,600†	-4.753e+7	-4.751e+7	0.025	98.59	1,311.8	-4.760e+7	–	0.149	92.51	568.5	-4.787e+7	2.414e+6	0.565	92.51	425.47
18	PEGASE 2869	–	–	3,600†	–	–	3,600†	-5.420e+7	-5.415e+7	0.090	98.38	1,529.8	-5.429e+7	-1.310e+6	0.174	92.38	600.66	-5.450e+7	-1.861e+6	0.378	92.38	425.17
19	PEGASE 2869	–	–	3,600†	–	–	3,600†	-5.394e+7	-5.393e+7	0.031	98.44	1,600.5	-5.310e+7	–	0.102	94.14	534.64	-5.412e+7	–	0.235	94.14	433.41
20	PEGASE 2869	–	–	3,600†	–	–	3,600†	-5.402e+7	-5.400e+7	0.027	98.22	2,755.3	-5.410e+7	-3.900e+6	0.147	92.94	399.14	-5.420e+7	-4.629e+6	0.1861	92.94	436.77
Avg			–	–		–	–			0.046		2,135.7			0.106		200.49			0.426		164.90
Max			–	–		–	–			0.354		2,755.3			0.323		600.66			2.646		436.77

† Solvers are terminated within 3600 seconds.

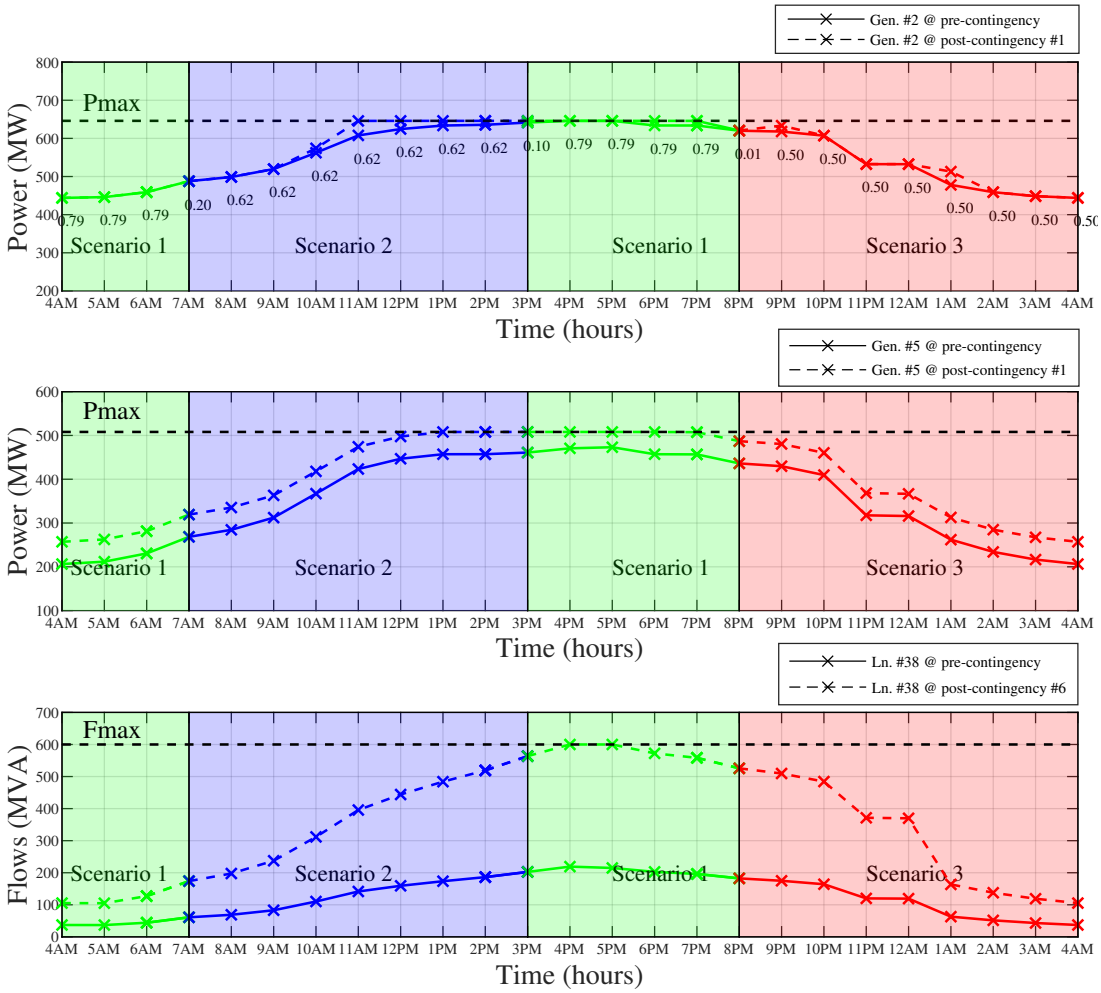

Fig. 3: New-England 39-bus (Experiment 1) 24-hr profile showing generator output and line flows. First from top: Gen. 2 base case and post-contingency power output showing transition probabilities across 3 scenarios. Second from top: Gen. 5 base case and post-contingency power output across 3 scenarios. Third from top: Line 38 basecase and post-contingency power flows across 3 scenarios.

must not exceed the maximum thermal limits, lines tend to become congested and in some cases reach critical levels.

0885-8950 (c) 2021 IEEE. Personal use is permitted, but republication/redistribution requires IEEE permission. See http://www.ieee.org/publications_standards/publications/rights/index.html for more information.
Authorized licensed use limited to: University of Texas at Arlington. Downloaded on April 01,2021 at 15:39:46 UTC from IEEE Xplore. Restrictions apply.

This article has been accepted for publication in a future issue of this journal, but has not been fully edited. Content may change prior to final publication. Citation information: DOI 10.1109/TPWRS.2021.3062203, IEEE Transactions on Power Systems

TABLE III: Generator data for New England 39-bus benchmark system (Experiment 1)

Unit	Gen. #1	Gen. #2	Gen. #3	Gen. #4	Gen. #5	Gen. #6	Gen. #7	Gen. #8	Gen. #9	Gen. #10	Wnd. #1	Wnd. #2	Wnd. #3
α_{tg}^{sqr} ($/MW^{2}h)	0.0026	0.0022	0.0013	0.0018	0.0009	0.002	0.0018	0.0019	0.0038	0.0026	0	0	0
α_{tg}^{lin} ($/MWh)	20.68	28.78	7.85	24.01	15.09	14.71	22.39	31.65	10.35	25.52	20	20	20
ζ_{tg} ($/h)	821.47	259.33	338.63	497.22	811.92	501.13	321.60	527.17	559.40	430.24	20	20	20
$\zeta_{tg}^{\uparrow}$ ($/h)	1,118.1	6,622.1	5,054	4,050.1	1,519.5	3,868.6	2,874	2,628	7,510.2	4,147.5	0	0	0
$\zeta_{tg}^{\downarrow}$ ($/h)	142.86	400.04	720	232.24	829.78	355.36	363.82	263.39	713.77	155.98	0	0	0
μ_{tg}^{+}, μ_{tg}^{-} ($/MWh)	4.13	5.75	1.56	4.80	3.01	2.94	4.47	6.32	2.07	5.10	4	4	4
η_{tg}^{+}, η_{tg}^{-} ($/MWh)	4.30	5.82	3.66	6.64	1.35	7.19	5.46	4.37	1.71	6.16	4	4	4
β_{tg}^{+}, β_{tg}^{-} ($/MWh)	103.37	143.88	39.24	120.07	75.46	73.53	111.93	158.23	51.77	127.59	100	100	100
κ_g ($/MW^{2}h)	1.29	1.10	0.66	0.89	0.47	1	0.91	0.93	1.88	1.31	0	0	0
Pmax (MW)	1040	646	725	652	508	687	580	564	865	1100	100	100	100
Pmin (MW)	0	0	0	0	0	0	0	0	0	0	0	0	0
$m_g^{\uparrow}$ (h)	7	5	10	7	1	7	10	7	1	1	1	1	1
$m_g^{\downarrow}$ (h)	3	10	4	7	1	4	5	10	1	1	1	1	1
Initial state (h)	5	-3	-4	3	3	-1	1	4	4	-1	1	1	1

TABLE IV: Binary commitment decisions for New England 39-bus benchmark system (Experiment 1)

Cost: $604,856.05																								
Unit	1	2	3	4	5	6	7	8	9	10	11	12	13	14	15	16	17	18	19	20	21	22	23	24
Gen. #1	1	1	1	1	1	1	1	1	1	1	1	1	1	1	1	1	1	1	1	1	1	1	1	1
Gen. #2	0	0	0	0	0	0	0	1	1	1	1	1	1	1	1	1	1	1	1	1	1	1	1	1
Gen. #3	1	1	1	1	1	1	1	1	1	1	1	1	1	1	1	1	1	1	1	1	1	1	1	1
Gen. #4	1	1	1	1	1	1	1	1	1	1	1	1	1	1	1	1	1	1	1	1	1	1	1	1
Gen. #5	1	1	1	1	1	1	1	1	1	1	1	1	1	1	1	1	1	1	1	1	1	1	1	1
Gen. #6	0	0	0	1	1	1	1	1	1	1	1	1	1	1	1	1	1	1	1	1	1	1	1	1
Gen. #7	1	1	1	1	1	1	1	1	1	1	1	1	1	1	1	1	1	1	1	1	1	1	1	1
Gen. #8	1	1	1	1	1	1	1	1	1	1	1	1	1	1	1	1	1	1	1	1	1	1	1	1
Gen. #9	1	1	1	1	1	1	1	1	1	1	1	1	1	1	1	1	1	1	1	1	1	1	1	1
Gen. #10	1	1	1	1	1	1	1	1	1	1	1	1	1	1	1	1	1	1	1	1	1	1	1	1
Wnd. #1	1	1	1	1	1	1	1	1	1	1	1	1	1	1	1	1	1	1	1	1	1	1	1	1
Wnd. #2	1	1	1	1	1	1	1	1	1	1	1	1	1	1	1	1	1	1	1	1	1	1	1	1
Wnd. #3	1	1	1	1	1	1	1	1	1	1	1	1	1	1	1	1	1	1	1	1	1	1	1	1

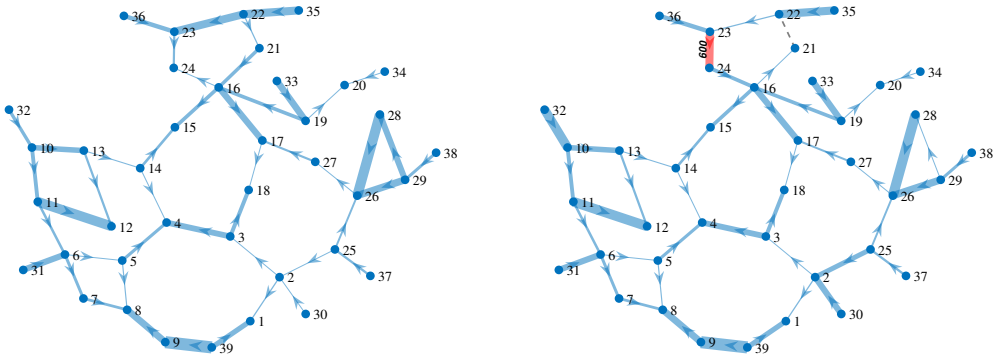

(a) Pre-contingency case @ 4PM , high wind penetration, no contingency

(b) Post-contingency case @ 4PM, high wind penetration, line contingency @ line 22 → 21. As a result of the contingnecy, line 23 → 24 is congested.

Fig. 4: Directed graph of New England 39-bus (Experiment 1) Pre and Post-contingencies

VI. Conclusions

In this paper, we study the SCUC problem under uncertainty by adopting a stochastic formulation proposed in [35]. The proposed method for tackling the computationally challenging problem is tested extensively on IEEE and PEGASE benchmark systems to establish its relative performance against two widely used off-the-shelf solvers, CPLEX and GUROBI and common-practice methods of relaxation, namely perspective and LP relaxations. It is shown that SDP relaxation consistently finds near-globally optimal solutions in each benchmark system under uncertain wind scenarios and with an extensive list of contingencies with up to 12,240 binary variables and 1,830,560 continuous variables.

References

[1] R. D. Zimmerman, C. E. Murillo-Sánchez, and R. J. Thomas, "Matpower: Steady-state operations, planning, and analysis tools for power systems research and education," *IEEE Transactions on Power Systems*, vol. 26, no. 1, pp. 12–19, 2011.

[2] E. National Academies of Sciences and Medicine, *Analytic Research Foundations for the Next-Generation Electric Grid*. Washington, DC: The National Academies Press, 2016.

[3] R. Johnson, S. Oren, and A. Svoboda, "Equity and efficiency of unit commitment in competitive electricity markets," *Utilities Policy*, vol. 6, pp. 9–19, 03 1997.

[4] R. H. Kerr, J. L. Scheidt, A. J. Fontanna, and J. K. Wiley, "Unit commitment," *IEEE Transactions on Power Apparatus and Systems*, vol. PAS-85, no. 5, pp. 417–421, 1966.

0885-8950 (c) 2021 IEEE. Personal use is permitted, but republication/redistribution requires IEEE permission. See http://www.ieee.org/publications_standards/publications/rights/index.html for more information.
Authorized licensed use limited to: University of Texas at Arlington. Downloaded on April 01,2021 at 15:39:46 UTC from IEEE Xplore. Restrictions apply.

This article has been accepted for publication in a future issue of this journal, but has not been fully edited. Content may change prior to final publication. Citation information: DOI 10.1109/TPWRS.2021.3062203, IEEE Transactions on Power Systems

[5] K. Hara, M. Kimura, and N. Honda, "A method for planning economic unit commitment and maintenance of thermal power systems," *IEEE Transactions on Power Apparatus and Systems*, vol. PAS-85, no. 5, pp. 427–436, 1966.

[6] R. C. Johnson, H. H. Happ, and W. J. Wright, "Large scale hydro-thermal unit commitment-method and results," *IEEE Transactions on Power Apparatus and Systems*, vol. PAS-90, no. 3, pp. 1373–1384, 1971.

[7] R. R. Shoults, S. K. Chang, S. Helmick, and W. M. Grady, "A practical approach to unit commitment, economic dispatch and savings allocation for multiple-area pool operation with import/export constraints," *IEEE Transactions on Power Apparatus and Systems*, vol. PAS-99, no. 2, pp. 625–635, 1980.

[8] F. N. Lee and Q. Feng, "Multi-area unit commitment," *IEEE Transactions on Power Systems*, vol. 7, no. 2, pp. 591–599, 1992.

[9] P. G. Lowery, "Generating unit commitment by dynamic programming," *IEEE Transactions on Power Apparatus and Systems*, vol. PAS-85, no. 5, pp. 422–426, 1966.

[10] J. D. Guy, "Security constrained unit commitment," *IEEE Transactions on Power Apparatus and Systems*, vol. PAS-90, no. 3, pp. 1385–1390, 1971.

[11] K. D. Le, J. T. Day, B. L. Cooper, and E. W. Gibbons, "A global optimization method for scheduling thermal generation, hydro generation, and economy purchases," *IEEE Power Engineering Review*, vol. PER-3, no. 7, pp. 25–26, 1983.

[12] M. L. Fisher, "Optimal solution of scheduling problems using lagrange multipliers: Part i," *Operations Research*, vol. 21, no. 5, pp. 1114–1127, 1973.

[13] D. Bertsekas, G. Lauer, N. Sandell, and T. Posbergh, "Optimal short-term scheduling of large-scale power systems," *IEEE Transactions on Automatic Control*, vol. 28, no. 1, pp. 1–11, 1983.

[14] J. A. Muckstadt and S. A. Koenig, "An application of lagrangian relaxation to scheduling in power-generation systems," *Operations Research*, vol. 25, no. 3, pp. 387–403, 1977.

[15] Yong Fu, M. Shahidehpour, and Zuyi Li, "AC contingency dispatch based on security-constrained unit commitment," *IEEE Transactions on Power Systems*, vol. 21, no. 2, pp. 897–908, 2006.

[16] ——, "Security-constrained unit commitment with ac constraints," *IEEE Transactions on Power Systems*, vol. 20, no. 3, pp. 1538–1550, 2005.

[17] X. Zhang, J. Zhao, and X. Chen, "A hybrid method of lagrangian relaxation and genetic algorithm for solving uc problem," in *2009 International Conference on Sustainable Power Generation and Supply*, April 2009, pp. 1–6.

[18] G. S. Lauer, N. R. Sandell, D. P. Bertsekas, and T. A. Posbergh, "Solution of large-scale optimal unit commitment problems," *IEEE Power Engineering Review*, vol. PER-2, no. 1, pp. 23–24, 1982.

[19] Y. Chen, A. Casto, F. Wang, Q. Wang, X. Wang, and J. Wan, "Improving large scale day-ahead security constrained unit commitment performance," *IEEE Transactions on Power Systems*, vol. 31, no. 6, pp. 4732–4743, 2016.

[20] G. B. Sheble and G. N. Fahd, "Unit commitment literature synopsis," *IEEE Transactions on Power Systems*, vol. 9, no. 1, pp. 128–135, 1994.

[21] A. S. Xavier, F. Qiu, F. Wang, and P. R. Thimmapuram.

[22] Jiaying Shi and S. S. Oren, "Wind power integration through stochastic unit commitment with topology control recourse," in *2016 Power Systems Computation Conference (PSCC)*, 2016, pp. 1–7.

[23] G. Morales-España, J. M. Latorre, and A. Ramos, "Tight and compact milp formulation for the thermal unit commitment problem," *IEEE Transactions on Power Systems*, vol. 28, no. 4, pp. 4897–4908, 2013.

[24] E. R. Bixby, M. Fenelon, Z. Gu, E. Rothberg, and R. Wunderling, "Mip: Theory and practice — closing the gap," in *System Modelling and Optimization*, M. J. D. Powell and S. Scholtes, Eds. Boston, MA: Springer US, 2000, pp. 19–49.

[25] J. Ostrowski, M. F. Anjos, and A. Vannelli, "Tight mixed integer linear programming formulations for the unit commitment problem," *IEEE Transactions on Power Systems*, vol. 27, no. 1, pp. 39–46, 2012.

[26] J. Lee, J. Leung, and F. Margot, "Min-up/min-down polytopes," *Discrete Optimization*, vol. 1, pp. 77–85, 06 2004.

[27] P. Damci-kurt, S. Küçükyavuz, D. Rajan, and A. Atamtürk, "A polyhedral study of production ramping," *Mathematical Programming*, vol. 158, no. 1-2, pp. 175–205, 07 2016.

[28] S. R. Shukla, S. Paudyal, and S. Kamalasadan, "Tight conic formulation of unit commitment problem and comparison with minlp/milp formulations," in *2018 IEEE Power Energy Society General Meeting (PESGM)*, 2018, pp. 1–5.

[29] J. Alemany, L. Kasprzyk, and F. Magnago, "Effects of binary variables in mixed integer linear programming based unit commitment in large-scale electricity markets," *Electric Power Systems Research*, vol. In Press, 03 2018.

[30] A. Frangioni and C. Gentile, "A computational comparison of reformulations of the perspective relaxation: Socp vs. cutting planes," *Operations Research Letters*, vol. 37, no. 3, pp. 206–210, 2009.

[31] X. Bai and H. Wei, "Semi-definite programming-based method for security-constrained unit commitment with operational and optimal power flow constraints," *IET Generation, Transmission Distribution*, vol. 3, no. 2, pp. 182–197, 2009.

[32] S. Fattahi, M. Ashraphijuo, J. Lavaei, and A. Atamtürk, "Conic relaxations of the unit commitment problem," *Energy*, vol. 134, no. C, pp. 1079–1095, 2017.

[33] J. Liu, C. D. Laird, J. K. Scott, J. Watson, and A. Castillo, "Global solution strategies for the network-constrained unit commitment problem with ac transmission constraints," *IEEE Transactions on Power Systems*, vol. 34, no. 2, pp. 1139–1150, 2019.

[34] F. Zohrizadeh, M. Kheirandishfard, A. Nasir, and R. Madani, "Sequential relaxation of unit commitment with ac transmission constraints," in *2018 IEEE Conference on Decision and Control (CDC)*, 2018, pp. 2408–2413.

[35] C. E. Murillo-Sánchez, R. D. Zimmerman, C. L. Anderson, and R. J. Thomas, "Secure planning and operations of systems with stochastic sources, energy storage, and active demand," *IEEE Transactions on Smart Grid*, vol. 4, no. 4, pp. 2220–2229, Dec 2013.

[36] A. Majumdar, G. Hall, and A. Ahmadi, "A survey of recent scalability improvements for semidefinite programming with applications in machine learning, control, and robotics," 08 2019.

[37] D. K. Molzahn, F. Dörfler, H. Sandberg, S. H. Low, S. Chakrabarti, R. Baldick, and J. Lavaei, "A survey of distributed optimization and control algorithms for electric power systems," *IEEE Transactions on Smart Grid*, vol. 8, no. 6, pp. 2941–2962, Nov 2017.

[38] A. Ahmadi and A. Majumdar, "Dsos and sdsos optimization: More tractable alternatives to sum of squares and semidefinite optimization," *SIAM Journal on Applied Algebra and Geometry*, vol. 3, 06 2017.

[39] B. Kirby and M. Milligan, "A method and case study for estimating the ramping capability of a control area or balancing authority and implications for moderate or high wind penetration," 01 2005.

[40] A. Frangioni and C. Gentile, "A computational comparison of reformulations of the perspective relaxation: Socp vs. cutting planes," *Oper. Res. Lett.*, vol. 37, no. 3, p. 206–210, May 2009.

[41] L. L. Garver, "Power generation scheduling by integer programming-development of theory," *Transactions of the American Institute of Electrical Engineers. Part III: Power Apparatus and Systems*, vol. 81, no. 3, pp. 730–734, 1962.

[42] J. A. Muckstadt and R. C. Wilson, "An application of mixed-integer programming duality to scheduling thermal generating systems," *IEEE Transactions on Power Apparatus and Systems*, vol. PAS-87, no. 12, pp. 1968–1978, 1968.

[43] A. I. Cohen and S. H. Wan, "A method for solving the fuel constrained unit commitment problem," *IEEE Transactions on Power Systems*, vol. 2, no. 3, pp. 608–614, 1987.

[44] H. D. Sherali and W. P. Adams, *Reformulation–Linearization Techniques for Discrete Optimization Problems*. New York, NY: Springer New York, 2013, pp. 2849–2896.

[45] MOSEK ApS, *The MOSEK optimization toolbox for MATLAB manual. Version 8.0.0.60*, 2016. [Online]. Available: https://docs.mosek.com/8.0/intro/index.html

[46] M. Grant and S. Boyd, "CVX: Matlab software for disciplined convex programming, version 2.1," http://cvxr.com/cvx, Mar. 2014.

[47] ——, "Graph implementations for nonsmooth convex programs," in *Recent Advances in Learning and Control*, ser. Lecture Notes in Control and Information Sciences, V. Blondel, S. Boyd, and H. Kimura, Eds. Springer-Verlag Limited, 2008, pp. 95–110, http://stanford.edu/~boyd/graph_dcp.html.

[48] R. D. Zimmerman, C. E. Murillo-Sanchez, and R. J. Thomas, "Matpower: Steady-state operations, planning, and analysis tools for power systems research and education," *IEEE Transactions on Power Systems*, vol. 26, no. 1, pp. 12–19, 2011.

[49] IBM, "Ilog cplex optimization studio v12.9.0," Mar. 2019.

[50] S. A. Kazarlis, A. G. Bakirtzis, and V. Petridis, "A genetic algorithm solution to the unit commitment problem," *IEEE Transactions on Power Systems*, vol. 11, no. 1, pp. 83–92, 1996.

[51] H. Kwon, J.-K. Park, D. Kim, J. Yi, and H. Park, "A flexible ramping capacity model for generation scheduling with high levels of wind energy penetration," *Energies*, vol. 9, p. 1040, 12 2016.

[52] Y.-H. Wan, "Wind power plant behaviors: Analyses of long-term wind power data," 01 2004.

0885-8950 (c) 2021 IEEE. Personal use is permitted, but republication/redistribution requires IEEE permission. See http://www.ieee.org/publications_standards/publications/rights/index.html for more information.
Authorized licensed use limited to: University of Texas at Arlington. Downloaded on April 01,2021 at 15:39:46 UTC from IEEE Xplore. Restrictions apply.

This article has been accepted for publication in a future issue of this journal, but has not been fully edited. Content may change prior to final publication. Citation information: DOI 10.1109/TPWRS.2021.3062203, IEEE Transactions on Power Systems

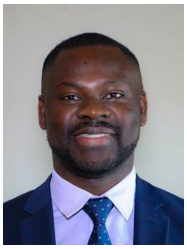

Edward Quarm Jnr. received his M.Sc. degree in systems control from Universite Grenoble Alpes, Grenoble, France in 2016. He is currently pursuing the Ph.D. degree in the Department of Electrical Engineering, University of Texas at Arlington, Arlington, TX, USA. His research interests include developing algorithms for optimization and control with applications in energy.

Ramtin Madani received the Ph.D. degree in electrical engineering from Columbia University, New York, NY, USA, in 2015. He was a Postdoctoral Scholar with the Department of Industrial Engineering and Operations Research at the University of California, Berkeley in 2016. He is an Assistant Professor with the Department of Electrical Engineering Department, University of Texas at Arlington, Arlington, TX, USA. His research interests include developing algorithms for optimization and control with applications in energy.

0885-8950 (c) 2021 IEEE. Personal use is permitted, but republication/redistribution requires IEEE permission. See http://www.ieee.org/publications_standards/publications/rights/index.html for more information.
Authorized licensed use limited to: University of Texas at Arlington. Downloaded on April 01,2021 at 15:39:46 UTC from IEEE Xplore. Restrictions apply.